

Template-directed colloidal crystallization

Alfons van Blaaderen*, Rene Ruel† & Pierre Wiltzius†

* FOM Institute for Atomic and Molecular Physics, Postbus 41883, 1009 DB Amsterdam, The Netherlands, and Van't Hoff Laboratory, Debye Institute, Utrecht University, Postbus 80051, 3508 TB Utrecht, The Netherlands

† Lucent Technologies, Bell Laboratories, 700 Mountain Avenue, Murray Hill, New Jersey 07974, USA

Colloidal crystals are three-dimensional periodic structures formed from small particles suspended in solution. They have important technological uses as optical filters¹⁻³, switches⁴ and materials with photonic band gaps^{5,6}, and they also provide convenient model systems for fundamental studies of crystallization and melting⁷⁻¹⁰. Unfortunately, applications of colloidal crystals are greatly restricted by practical difficulties encountered in synthesizing large single crystals with adjustable crystal orientation¹¹. Here we show that the slow sedimentation of colloidal particles onto a patterned substrate (or template) can direct the crystallization of bulk colloidal crystals, and so permit tailoring of the lattice structure, orientation and size of the resulting crystals: we refer to this process as 'colloidal epitaxy'. We also show that, by using silica spheres synthesized with a fluorescent core^{12,13}, the defect structures in the colloidal crystals that result from an intentional lattice mismatch of the template can be studied by confocal microscopy¹⁴. We suggest that colloidal epitaxy will open new ways to design and fabricate materials based on colloidal crystals and also allow quantitative studies of heterogeneous crystallization in real space.

Epitaxial growth of a thin crystalline layer onto a template consisting of an oriented single crystal is an important process in the development of electronic devices. For instance, in molecular

beam epitaxy careful control over reagent flow and temperature make it possible to achieve layer-by-layer growth of oriented crystal structures that can even be slightly out of equilibrium¹⁵. We have extended these ideas of template-directed crystallization to colloids, which are the ideal building blocks for photonic applications owing to their submicrometre sizes, self-organization and the possibility of chemically tailoring their properties. As a template we used a 500-nm-thick fluorescent polymer layer, with holes made with electron beam lithography (Fig. 1A). This thickness is close to the particle radius (525 nm) of the fluorescent silica spheres (fluorescent core: 200 nm). The interparticle forces are made hard-sphere-like by matching the refractive index of the solvent mixture to that of the spheres, minimizing van der Waals forces, and by increasing the ionic strength to such values that double-layer repulsion occurs over distances much smaller than the particle radius. Controlled layer-by-layer growth was achieved by slow sedimentation of the spheres onto the substrate from a volume fraction of particles well below the 50% volume fraction of homogeneous crystallization of hard-spheres⁷⁻¹⁰.

Experimentally, hard-sphere-like colloidal dispersions are known to crystallize with a random stacking of close packed planes^{7-10,16}. Theoretically, it is not clear what the thermodynamic equilibrium phase is; also, computer simulations have not been able to determine whether face-centred cubic (f.c.c., with stacking order ABC), hexagonal close packed (h.c.p., stacking ABA) or random stacking is favoured¹⁷. It is known, however, that thermodynamically these structures have almost the same free energy. As suggested by others¹⁶, we found in this work that crystals that form through sedimentation have a random stacking with the close-packed planes perpendicular to gravity. Strictly speaking, a random stacked structure of close-packed planes is not a crystal, because of the randomness in one crystallographic direction. However, when a colloidal crystal was grown normal to a pattern of holes commensurate with the (100) plane of a f.c.c. crystal (Fig. 1A inset), a pure f.c.c. crystal was formed (Fig. 1B, C). By use of light scattering, we found that the f.c.c. crystal extended as far as the sedimented layer is thick (several millimetres). Also, the single crystals grew as large as the size of the pattern.

The reason for the formation of the f.c.c. crystal is that the (100) face can induce a three-dimensional structure: there is only one possible way the second layer can be placed on the holes created by the first layer. In other words, there is no twinning possibility along this growth direction (twinned crystals share a common set of atoms, but have a different orientation of their (otherwise similar) lattices). A sphere dropping into a hole 500 nm deep loses 0.6 kT in gravitational energy, where k is Boltzmann's constant and T the absolute temperature. Apparently, the small increased likelihood of a square symmetry as induced by the pattern shown in Fig. 1 is enough to start of the crystal growth with the (100) plane instead of the (111) hexagonal plane which is the densest crystal plane. For the growth of the crystal, the balance between diffusion and sedimentation is important. This balance is described by the Peclet number $Pe = m_b g R / kT$, where m_b is the buoyant mass of a particle with radius R and g is the gravitational acceleration. Pe is defined as the ratio of the time it takes a particle to diffuse over a distance R and the time it takes to settle over the same distance; in this work $Pe \approx 1$. For the crystal layers close to the template, the situation is very different at the end of the growth. Here the weight of several thousand layers exerts such a pressure that osmotic pressure can only balance this at a crystal volume fraction experimentally indistinguishable from close packing, 0.74.

The growth of macroscopic f.c.c. single crystals on the (110) plane, which is even less dense than the (100) plane and also has no twinning directions, was also possible. These results make it likely that the growth of pure hexagonal close-packed (h.c.p.) crystals on a non-dense h.c.p. plane that has no associated twinning direction will be feasible as well.

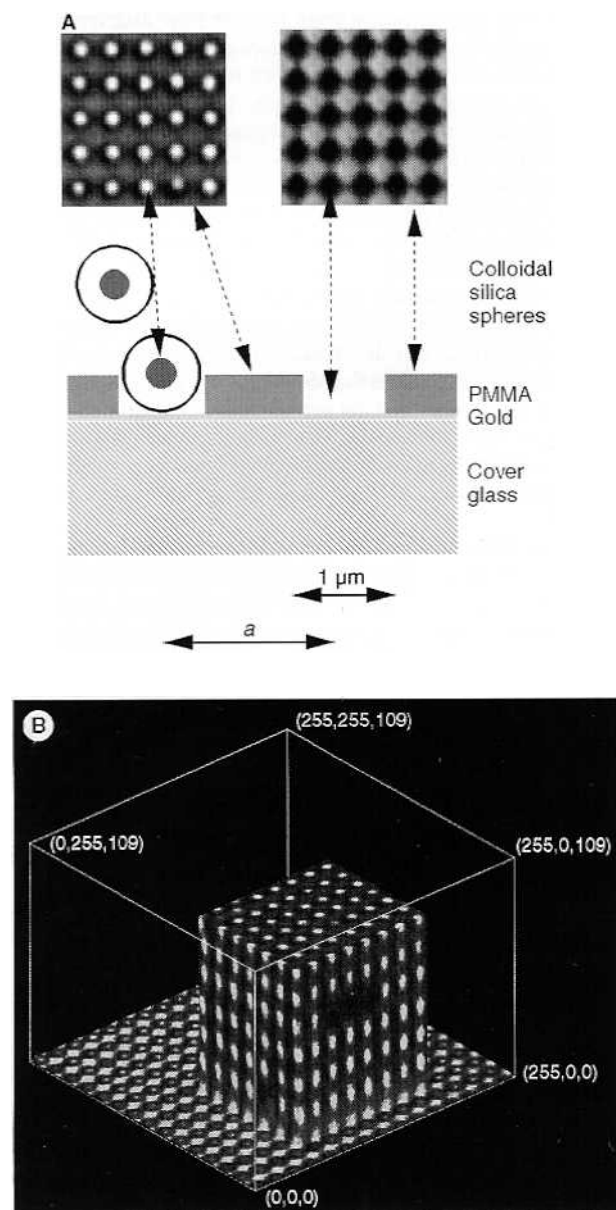


Figure 1 Face-centred cubic (f.c.c.) hard-sphere-like colloidal crystals grown on a (100) f.c.c. template created in a polymer layer. **A**, Schematic diagram of the colloidal epitaxy procedure (bottom) and two confocal micrographs (top) showing the fluorescently labelled polymer template with (left) and without (right) a first layer of spheres. **B**, Cut-out of a three-dimensional stack of confocal sections ($256 \times 256 \times 120$ voxels, three-dimensional picture elements, $16.5 \mu\text{m} \times 16.5 \mu\text{m} \times 10.5 \mu\text{m}$) on top of the polymer template. **C**, computer-generated picture of the experimental data set shown in **B** and with the sphere positions obtained as described in ref. 14. Methods: The silica spheres were dispersed in a refractive-index-matched mixture of water and glycerol (16 wt% glycerol) with 0.01 M LiCl and had starting volume fractions of 1% and 5%; no differences were found in this range of concentration. (The total radius of the silica spheres was 525 nm, of which the fluorescent core comprised 200 nm.) The dyed (pyromethene 580, 10^{-3} wt%) polymer (polymethylmethacrylate, PMMA) was spin-coated (500-nm thick) on a cover slip (no. 1; $170 \mu\text{m}$ thick) on which a thin layer of gold (5 nm) was sputtered. The pattern of holes (400×400) was created with electron beam lithography. The fluorescence confocal micrographs were made with a Multiprobe 2001 (Molecular Dynamics) confocal apparatus; see ref. 14 for further details. The distance of closest approach of the spheres was 1,105 nm in a glass and 1,110 nm in a crystal after full sedimentation. These values are close to the distances reported in 0.1 M dimethylformamide¹⁴ and show that the colloidal crystals are almost completely compressed as explained in the text.)

In Fig. 2 and Table 1 we show the defect structures that result from a mismatch of the (100) f.c.c. lattice parameter a (expressed in particle diameters). At small mismatches ($1.1 < a < 1.2$), the first few layers start out with a perfect square symmetry, but in subsequent layers the symmetry changes into hexagonally packed and randomly stacked layers through the gradual introduction of defects similar to Fig. 2A and B. At larger mismatch ($a \approx 1.2$) the template imposes a square symmetry in the first layer only in certain bands (Fig. 2C). Again, several layers higher, random stacked (111) planes are found everywhere. A similar structure is found for heteroepitaxial growth of CdTe on GaAs(100). Because of a large mismatch

(in one direction 14.6%) CdTe grows with (111) planes on the (100) template¹⁸. Of course, the interaction potential in this system is not hard-sphere-like, but the structural resemblances are striking. With still larger mismatch even the first layers is (defect-rich) hexagonal and the layers above stack again randomly, similar to Fig. 2D. For $a = \sqrt{2}$ the square lattice is, after rotation of 45° , commensurate with the original (100) plane with $a = 1$. The missing holes (Fig. 2E) in the first layer do not prevent the growth of a full f.c.c. crystal on the template. Around this lattice mismatch, the defect structures are similar to those found close to $a = 1$ (Table 1). It is interesting to note that at no lattice spacing was a body-centred (b.c.c.) crystal,

Table 1 Crystal structure formed on f.c.c. (100) plane as function of lattice spacing a

| a | ~ 1.0 | 1.1-1.2 | ~ 1.2 | 1.2-1.3 | ~ 1.3 | 1.3-1.4 | $\sim \sqrt{2}$ | 1.4-1.5 | ~ 1.5 | 1.5-2.0 |
|-------------------------|-------------------|---------|------------|---------|------------------|----------------|-----------------|---------|------------|----------------|
| Symmetry of first layer | □ (Fig. 1B, C) | □ | □/▷ | ▷ | ◇/▷ (Fig. 2C) | ◇ (Fig. 2A) | ◇ (Fig. 2E) | ◇ | ◇/▷ | ▷ (Fig. 2D) |
| Symmetry of tenth layer | □ (Fig. 1B, C) | ▷ | ▷ | ▷ | ▷ | ▷ (Fig. 2B) | ◇ | ▷ | ▷ | ▷ |

Here the lattice spacing a is given in multiples of the particle diameter. The symbols represent the symmetry of the crystalline layer: square (□), hexagonal (▷), 45° rotated square, see text (◇).

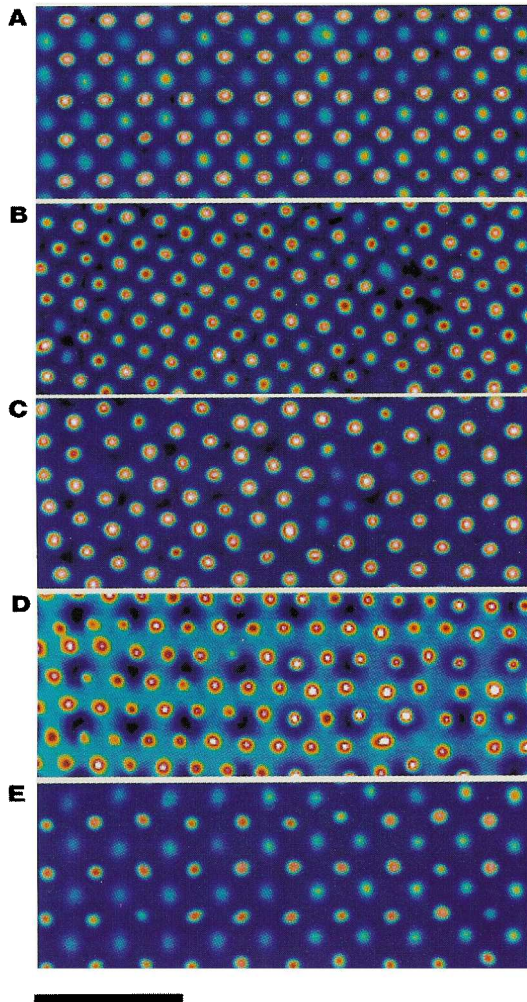


Figure 2 Local crystal plane symmetry of crystals grown on f.c.c. (100) planes with different lattice spacing a (given in multiples of the particle diameter). **A**, Part of optical section showing (100) symmetry of the first and the (first visible) second layer of spheres on a template with $a = 1.35$. **B**, As **A**, but ten layers above the template showing defect-rich hexagonal (111) symmetry. **C**, First layer above the template with $a = 1.3$ showing bands of (111) symmetry (left) and (100) symmetry (right). **D**, First layer of spheres with $a = 1.6$ showing a defect-rich hexagonal symmetry. **E**, First and second layers on a template with a close to $\sqrt{2}$ showing (100) symmetry, but rotated 45° compared to the crystal shown in Fig. 1. Scale bar, $5\ \mu\text{m}$. The 'rainbow' false-colour table allows for easy visualization of which particle belongs in which layer and also makes it possible to recognize the template.

which has a (100) crystal plane with the same symmetry, formed. Probably, the difference in free energy of the less-dense b.c.c. crystal is too far off to be induced by the template.

Figure 3 gives another example of the manipulative possibilities of colloidal epitaxy. A simple change in the spacing between two adjacent (100) f.c.c. planes determines whether the (100) plane continues over the unpatterned region or whether a stack of (111) planes will form between the two f.c.c. crystals. Structures like these are important for the creation of optical wave guides.

Here we have shown that with colloidal epitaxy it is possible to create large hard-sphere f.c.c. single crystals oriented along crystal directions without twinning. It has also been shown that tailored crystals with different crystal orientations can be grown next to each other. Hard-sphere-like crystals are important for applications,

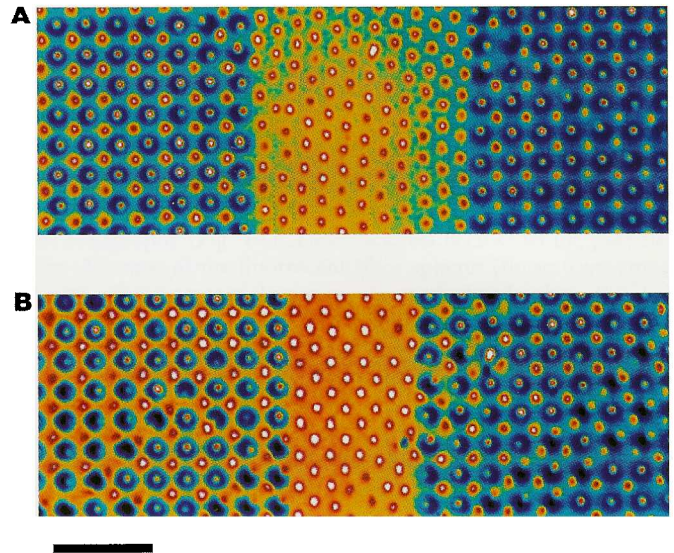


Figure 3 Confocal micrographs of the first layer of spheres on the (100) f.c.c. template with a close to $\sqrt{2}$ but with different distances between two templated regions (left, right): **A**, 11 sphere diameters: a hexagonal symmetry appears between the (100) faces. **B**, 7 sphere diameters: the square symmetry continues over the unpatterned polymer layer. Scale bar, $5\ \mu\text{m}$.

because after slow drying these crystals can be turned into connected dielectric structures. In the case of particles with a silica coating this can be achieved through a mild sintering around 100°C which forms chemical siloxane bonds between the particles. Subsequently, the solvent can be changed without changing the dielectric structure.

Moreover, particles that interact with a hard-sphere-like potential provide the simplest model system with which to study quantitatively the defects that form after mismatching of the template lattice. Such mismatches can almost never be avoided in atomic heteroepitaxy. There is no reason, however, why our technique could not be extended to charged spheres as well. In this case ionizable groups would have to be present on the template. Larger templates could be more easily created with other methods like photolithography or, as recently has been demonstrated with feature sizes of 25 nm thickness, with imprint lithography¹⁹. Further work is necessary to determine the influence of the sedimentation rate and volume-fraction on the epitaxial structures; preliminary experiments have already given indications of an interesting growth mechanism. For photonic bandgap materials it would be advantageous if the method could be extended to binary crystals as well. The use of a template could help systematic study of heterogeneous crystallization by observing the effects of the template under conditions at, or close to, homogeneous crystallization. □

Received 11 July; accepted 25 November 1996.

1. Flaugh, P. L., O'Donnell, S. E. & Asher, S. A. *Appl. Spectrosc.* **38**, 847–850 (1984).
2. Kamenetzky, E. A., Mangiocco, L. G. & Panzer, H. P. *Science* **263**, 207–210 (1994).
3. Sunkara, H. B., Jethmalani, J. M. & Ford, W. T. *Chem. Mater.* **6**, 362–364 (1994).
4. Chang, S., Liu, L. & Asher, S. A. *J. Am. Chem. Soc.* **116**, 6739–6744 (1994).
5. Vos, W. L. *et al. Phys. Rev. B* **53**, 16231–16235 (1996).
6. Tarhan, I. I. & Watson, G. H. *Phys. Rev. Lett.* **76**, 315–318 (1996).
7. Ackerson, B. J. & Schätzle, K. *Phys. Rev. E* **52**, 6448–6460 (1995).
8. Pusey, P. N. *et al. Phys. Rev. Lett.* **63**, 2753–2757 (1989).
9. Pusey, P. N. & van Meegen, W. *Nature* **320**, 340–342 (1986).
10. Harland, J. L., Henderson, S. M., Underwood, S. M. & van Meegen, W. *Phys. Rev. Lett.* **75**, 3572–3575 (1995).
11. Palberg, T., Mönch, W., Schwarz, J. & Leiderer, P. *J. Chem. Phys.* **102**, 5082–5087 (1995).
12. van Blaaderen, A. & Vrij, A. *Langmuir* **8**, 2921–2931 (1993).
13. Verhaegh, N. A. M. & van Blaaderen, A. *Langmuir* **10**, 1427–1438 (1994).
14. van Blaaderen, A. & Wiltzius, P. *Science* **270**, 1177–1179 (1995).
15. Parker, E. H. C. (ed.) *The Technology and Physics of Molecular Beam Epitaxy* (Plenum, New York, 1985).

16. Davis, K. E., Russel, W. B. & Glantsching, W. J. *Science* **245**, 507–510 (1989).
17. Frenkel, D. & Ladd, A. J. C. *J. Chem. Phys.* **81**, 318–3193 (1984).
18. Bourret, A., Fuoss, P., Geuillet, G. & Tatarenko, S. *Phys. Rev. Lett.* **70**, 311–314 (1993).
19. Chou, S. Y., Krauss, P. R. & Renstrom, P. J. *Science* **272**, 85–87 (1996).

Acknowledgements: We thank C. A. Murray for discussions and D. Frenkel for a critical reading of the manuscript. This work is part of the research programme of the Foundation for Fundamental Research of Matter (FOM) with financial support of the Netherlands Organization for Scientific Research (NWO).

Correspondence should be addressed to A.v.B. (e-mail: A.vanBlaaderen@chem.ruu.nl).